# Hydration of Valine−Cation Complexes in the Gas Phase: On the Number of Water Molecules Necessary to Form a Zwitterion

**Rebecca A. Jockusch, Andrew S. Lemoff, and Evan R. Williams***

*Department of Chemistry, University of California, Berkeley, California 94720-1460*

*Received: August 28, 2001*

The stepwise hydration of valine−alkali metal ion complexes, Val·$M^+(H_2O)_n$, $n = 2-6$, M = Li, Na, and K, is investigated using both theory and experiment. Experimentally, the rate of water loss from the valine clusters is measured using blackbody infrared radiative dissociation. The kinetics for the loss of one water molecule from these clusters are compared to those from model clusters of known zwitterionic vs nonzwitterionic structure. Both theory and experiment indicate that the structure of Val·$Li^+(H_2O)_2$ is very similar to that of the singly and nonhydrated complexes investigated previously; the lithium is coordinated between the nitrogen and carbonyl oxygen of nonzwitterionic valine, and the water molecules interact solely with the metal ion. The third water molecule changes the structure of the Val·$Li^+$ cluster significantly. The metal ion coordinates to the C-terminal end of zwitterionic valine and to two of the water molecules. The third water molecule hydrogen bonds to the protonated N terminus of valine. Thus, the third water molecule is the first one that interacts directly with the valine, and this stabilizes the zwitterionic form of valine over the nonzwitterionic form. The dissociation of the sixth water molecule from the valine cluster is slower than that of the fifth, indicating that the cluster with six waters is especially stable relative to the cluster with five water molecules. This provides further support for zwitterionic valine in the presence of only a limited number of water molecules. For M = Na, two water molecules changes the metal binding position from NO coordination to the C terminus of valine. The experiment is unable to distinguish the zwitterionic vs nonzwitterionic character of valine in this complex, but theory indicates the nonzwitterion form. As is the case with lithiated clusters, Val·$Na^+(H_2O)_6$ is more stable than Val·$Na^+(H_2O)_5$. Computational results for M = K predict that the most stable conformation of Val·$K^+(H_2O)_2$ resembles Val·$Na^+(H_2O)_2$, whereas the kinetic data for the sodiated and potassiated clusters, although inconclusive, suggest the zwitterion form. The stepwise hydration studies presented here indicate that very few water molecules are necessary to cause valine to adopt its solution-phase zwitterionic structure.

## Introduction

Despite water's central role in biology, the nature of water−biomolecule interactions remains nebulous. The hydrophobic effect is thought to be one of the driving forces in the folding of proteins into their compact three-dimensional structure.[1] However, there are examples of proteins that are active in nonpolar solvents.[2] There is also extensive evidence indicating that several proteins can form compact structures in the gas phase, although detailed information about these compact structures remains illusive.[3−6] In addition to general solvation effects, water is also known to mediate many biochemical reactions.[7] The environment in which biomolecules function is not only defined by water molecules; the presence of metal ions also has a great effect. Gas-phase studies can be used to separate these environmental effects from the intrinsic properties of the biomolecules. For example, the amino acid with the highest helix-forming propensity in solution is alanine.[8] However, protonated polyalanine does not adopt a helical conformation in the gas phase.[9] If the proton is replaced by an alkali metal ion, the peptide forms a helix; that is, it adopts its solution-phase conformation.[10] The stable gas-phase helix is presumably due to the favorable electrostatic interaction between the metal ion and the dipole of the helix. These and other experiments[11−13] indicate that some aspects of the solution-phase structure of biomolecules can exist in the gas phase. Of equal importance, from differences in the gas-phase and solution-phase structure, one can learn directly about the influence of water on biomolecular structure.

It should also be possible to stabilize a solution-phase structure in the gas phase by the attachment of specific water molecules to the gas-phase biomolecule ion, i.e., by hydration of the gas-phase ion. Extensively hydrated gas-phase biomolecule ions can be formed by electrospray ionization,[14−16] but little detailed information about the structures of these hydrated ions has been reported. In principle, the gap in our understanding between the gas-phase and solution-phase properties of biomolecules can be bridged by investigating how water changes the biomolecule structure, one water molecule at a time.

The structure of amino acid-cation complexes provides a simple model for biologically relevant hydration studies. In solution over a wide pH range, all amino acids are zwitterions with a protonated N terminus and/or side chain and a deprotonated C terminus and/or side chain. The dipole thus formed is stabilized in solution through interactions with polar solvent molecules and by the electric field of nearby counterions. In the absence of these external stabilizing forces, i.e., for naked molecules in the gas phase, the ground state form of all amino acids is nonzwitterionic. For glycine (Gly), the zwitterionic form

* To whom correspondence should be addressed.

10.1021/jp013327a CCC: $20.00 
Published on Web 10/25/2001

is calculated to be ~19 kcal/mol higher in energy than the nonzwitterionic form.[17] Calculations indicate that there is no barrier to proton transfer,[17−20] so the zwitterionic form is not stable, and this form has not been observed experimentally.[21−23] The zwitterionic and nonzwitterionic forms of the most basic amino acid, arginine (Arg), are more comparable in energy.[24,25] However, high-level calculations indicate that the nonzwitterionic form is ~1 kcal/mol more stable than the zwitterionic form.[25] Cavity ring down experiments show no evidence for the existence of zwitterionic Arg.[26]

Electrostatic interactions with metal ions significantly stabilize zwitterionic forms of amino acids relative to nonzwitterionic forms. Calculations on Gly−alkali-metal-cation ($M^+$) complexes predict that the nonzwitterionic Gly·$M^+$ complexes remain more stable than their zwitterionic counterparts by just 1−3 kcal/mol,[27−30] and ion mobility experiments indicate that Gly·$Na^+$ is nonzwitterionic.[29] Both experiments and theory on Arg·$M^+$ complexes indicate that as the size of the counterion increases, the zwitterionic complex is stabilized relative to the nonzwitterion form. In Arg·$K^+$, Arg·$Rb^+$, and Arg·$Cs^+$, Arg is zwitterionic.[31]

Several computational studies have investigated the stabilizing properties of individual water molecules on the zwitterionic form of amino acids. With two correctly placed water molecules, the glycine zwitterion is a local minimum on the potential energy surface; however, this structure is significantly higher in energy (~12 kcal/mol) than the most stable nonzwitterionic structure.[20] With three water molecules, recent calculations suggest that the zwitterion and nonzwitterion forms become degenerate.[32] Another computational investigation focused on accurate reproduction of the spectroscopic behavior of aqueous alanine. Spectra calculated for clusters of alanine with four water molecules reproduced many features observed in aqueous experimental data that are missing from calculated spectra of unhydrated alanine.[33]

Although several theoretical studies have addressed the structure of hydrated gas-phase amino acids, little experimental work has been reported. The binding of single water molecules was used to probe the structures of unhydrated protonated glycine and lysine,[34] and several recent experimental investigations have focused on hydration of amino acid analogues and small peptides.[34−40] Thermochemical data on the binding of water to small proteins has also been reported.[41]

We recently began an investigation into the combined effects of alkali cation adduction and hydration on amino acid structure by examining Val·$M^+$ and Val·$M^+(H_2O)_1$ clusters using both experiments and computation.[42] These studies showed that for M = Li and Na, the valine has a nonzwitterionic structure, and the metal ion is coordinated to both the nitrogen and carbonyl oxygen (NO coordination) of the amino acid. The addition of a single water molecule to Val·$M^+$ does not change the structure of valine, nor does it effect the relative energetics of the zwitterionic vs nonzwitterionic form. Potassium was shown to bind quite differently to valine than lithium or sodium. The most stable structure of the unhydrated complex has the metal coordinated between the two oxygens (OO coordination) of valine. In the experiment, we were not able to unambiguously determine whether the valine adopted a zwitterionic or nonzwitterionic structure with potassium. However, relatively high-level theoretical calculations indicate that the cluster containing the nonzwitterionic valine is 3.0 kcal/mol more stable than the salt-bridge structure in which valine is a zwitterion.

Here, we extend our studies to include higher states of hydration and investigate the structures of Val·$M^+(H_2O)_n$, $n$ = 2−6, M = Li, Na, and K. We follow the experimental approach developed in our previous work. The structure of these clusters is probed by comparing the relative kinetics for the evaporation of the $n$th water molecule from clusters containing valine to that from clusters containing isomers of valine which are either zwitterionic or nonzwitterionic. This is combined with a computational investigation of a wide range of possible structures for the $n$ = 2 and 3 clusters. The structure of Val·$Li^+(H_2O)_6$ is also explored, using less extensive computations, because of its special stability observed experimentally.

## Experimental Methods

**Chemicals.** Valine (Val) was obtained from Sigma Chemical Co. (Saint Louis, MO). The hydrochloride salt of alanine ethyl ester (AlaOEt) and the monohydrate and hydrochloride salt of betaine (Bet) were obtained from Aldrich Chemical Co. (Milwaukee, WI). Hydroxides and chloride salts of Li, Na, and K were purchased from Fisher Scientific (Fair Lawn, NJ). All chemicals were used as purchased. Electrospray solutions were made to 1 mM amino acid (or amino acid analog) and 1 mM metal ion using deionized water. Good signal was obtained from these high-molarity solutions. By comparison, electrospray solutions are typically about 100 times less concentrated. Chloride salts were used to form hydrated Val·$M^+$ and Bet·$M^+$ clusters, whereas metal hydroxides gave much better signal for the AlaOEt·$M^+$ clusters. Separate experiments comparing the evaporation rates of water from Bet·$M^+$ clusters made with metal hydroxide and metal chloride salts were performed. No differences in evaporation rates were observed, indicating that the source of the metal ion and the presence of chloride vs hydroxide in the electrospray solution does effect the dissociation kinetics of the isolated ions.

**Mass Spectrometry.** Tips for nanoelectrospray ionization were pulled from 0.78 mm inner diameter borosilicate capillaries to a diameter of ~3−5 $\mu$m using a Flaming−Brown micropipet puller (Sutter Instruments model P-87, Novato, CA). A platinum wire inserted down the center of the nanospray tips is used as an electrode and is held at a potential of ~1 kV. Electrosprayed ions are trapped in the ion cell of our home-built Fourier transform mass spectrometer that has a 2.7 T superconducting magnet. Details of our instrument can be found elsewhere.[43,44] After a period of 2−5 s during which ions are accumulated in the ion cell, a mechanical shutter is closed to stop further ions from entering. Nitrogen gas ($2 \times 10^{-6}$ Torr) is pulsed into the ion cell during the load period and for a short time (1−2 s) afterward to assist in ion trapping. After a 2 s pump-down delay, the ion cell returns to a base pressure of $< 5 \times 10^{-9}$ Torr. Unwanted ions are ejected from the cell using a series of single frequency, stored waveform inverse Fourier transform (SWIFT) and chirp excitation waveforms. The cluster of interest is then allowed to react for times ranging from 0 to 300 s. For experiments involving a heated cell, the temperature of the entire vacuum chamber is raised by using electrically resistive heating blankets located on the outside of the chamber. For experiments involving a cooled cell, the copper jacket surrounding the cell is cooled to a uniform temperature.[44] This is done by regulating the opening and shutting of a solenoid that controls the flow of liquid nitrogen around the outside of the copper jacket. Prior to all experiments, the temperature is allowed to equilibrate overnight (> 8 h) to ensure that the ions are exposed to a steady-state radiative energy distribution from infrared photons emitted from the walls of the copper jacket and vacuum chamber. Following the variable reaction delay, the product ions are excited for detection using a frequency sweep with a rate of

2200 Hz/$\mu$s. A detection bandwidth of 1778 kHz is used. Data are acquired using an Odyssey data system (Finnegan MAT, Bremen, Germany). For all clusters of specific hydration number and M, the experimental sequence (load time and isolation waveforms) was optimized for the isomeric cluster that gave the poorest signal, typically AlaOEt·$M^+(H_2O)_n$. The same experimental sequence was then used for the remaining isomeric clusters, and these sets of experiments were done on the same day, usually following each other. This was done in order to ensure that dissociation of the isomeric clusters (i.e., those with the same metal ion and extent of hydration) was done under as identical experimental conditions as possible.

Although the copper jacket is at a known temperature, there are holes in the jacket that allow radiation from other parts of the vacuum chamber to enter the ion cell and interact with the ions. For this reason, the internal energy distribution of the ions is not well characterized for the experiments performed in the cooled cell. Therefore, we will refer to the temperature of the copper jacket as the nominal temperature of the ion cell.

**Computational Details.** Starting structures for higher-level calculations were made using a combination of conformational searching and chemical intuition. Structures of AA·$Li^+(H_2O)_n$, $n$ = 2 and 3 clusters were generated using Monte Carlo conformation searching with the AMBER* force field and the Maestro suite of programs (Schrodinger, Inc., Portland, OR). For the initial search, no constraints were placed on the molecules, and 1000 conformations were generated in order to explore as wide a range of structures as possible. All structures from the initial search that were within 5 kcal/mol of the lowest-energy conformer were examined to develop chemical intuition as to the possible AA conformations and modes of metal ion and water binding. The AMBER* force field appears to minimize Bet to the wrong structure; the carboxylate group is rotated 90° from the minimized structures at higher levels of theory. For Bet-containing clusters, Bet was forced to adopt the correct higher-level structure and constrained to this geometry. A subsequent round of conformational searching was performed with AA geometries constrained to representative ones found in the first search (and the manufactured betaine structure). All structures that were within 5 kcal/mol of the minimum structure involving the same AA geometry were examined. Starting structures for higher-level calculations were chosen from this second group of structures with fixed AA geometry. In several instances, additional structures which were more than 5 kcal/mol less stable than the lowest-energy structure were also chosen. In no instance were these additional higher energy structures found to be the most stable structure at higher levels of theory. Additional conformational searching with M = K was performed in order assess whether the candidate conformations determined for M = Li were valid for larger metal ions. Most conformations selected for M = Li (including several of the higher-energy ones) were low-energy conformations for M = K with the AMBER* force field. However, there were several additional M = K structures within the 5 kcal/mol range. Thus, although the cluster conformations for the smaller metal ions represent a relatively thorough search of the potential energy surface, it is possible that some low-energy conformations for the potassiated clusters were missed.

Many starting structures for Val·$Li^+(H_2O)_6$ clusters were taken directly from the initial unconstrained conformation search. For clusters containing nonzwitterionic valine (VN), there were 46 structures within 5 kcal/mol. Only the three lowest energy conformers were selected for higher-level calculations. This corresponded to all of the structures within 1 kcal/mol of the minimum. For clusters containing zwitterionic valine (VZ), there were 12 structures that were within 5 kcal/mol. The six lowest-energy clusters with VZ were selected for higher level calculations. This corresponded to all of the structures within 4 kcal/mol of the minimum for the VZ isomer. Nine additional VZ conformers were selected from among the higher-energy structures from the initial conformation search and from subsequent searches with constrained geometries. None of these additional structures was the lowest-energy VZ conformer found, although several were within 5 kcal/mol of the most stable structure.

After the selection of starting structures from mechanics calculations, hybrid method density functional calculations (B3LYP) were performed using Jaguar versions 3.5 and 4.0 (Schrodinger, Inc., Portland, OR) with increasingly large basis sets. For M = Li and Na, the basis sets used were 6-31G* full optimization, 6-31+G* full optimization, and 6-311++G** single-point energy calculations at the 6-31+G*-optimized geometry. For M = K, the basis sets used were LACVP* full optimization, LACVP+* full optimization, and LACVP++** single-point calculations at the LACVP+*-optimized geometry. The LACVP basis includes an effective core potential for potassium and uses the 6-31G basis for the other atoms present.[45] Second-order Möller−Plesset perturbation theory (MP2) calculations using Gaussian 98 (Gaussian, Inc., Pittsburgh, PA) were done for a limited number of Val·$Li^+(H_2O)_2$ and Val·$Li^+(H_2O)_3$ conformers.

Starting structures for sodiated clusters were generated from lithiated cluster structures. If the conformation of the lithiated cluster did not change significantly after B3LYP/6-31G* optimization, the lithium of the B3LYP/6-31G*-optimized cluster was replaced by sodium to generate the analogous sodiated cluster conformation. Similarly, the B3LYP/6-31G*-optimized geometry of the sodiated cluster was used as the starting structure for the B3LYP/LACVP* calculation of the analogous potassiated cluster. In some cases, the conformation changed significantly during the initial B3LYP calculation. In these instances, the original AMBER* structure was used as the starting structure for the sodiated and/or potassiated clusters. This was done to increase efficiency while attempting to circumvent the possibility that energetically competitive conformations for M = Na and K might be lost because it was not stable for M = Li. Several additional structures for B3LYP calculations of potassiated clusters were selected from AMBER* conformation searching performed directly on potassiated clusters. Nuclear coordinates for all structures shown in this paper are listed in Table S1.

## Results and Discussion

Structure is inferred from the experimental results by comparing the relative dissociation kinetics for the evaporation of the $n$th water molecule from Val·$M^+(H_2O)_n$ clusters and its isomeric analogues activated by blackbody infrared radiative dissociation (BIRD). The measured dissociation rate for the valine-containing cluster is compared to that of clusters containing isomers of valine, one that is zwitterionic, the other nonzwitterionic. The isomers used for this study are alanine ethyl ester (AlaOEt), a nonzwitterion, and betaine (Bet), a zwitterion. The structures of AlaOEt, Bet, and Val (generically abbreviated AA for amino acid or amino acid analogues) are shown in Scheme 1.

The comparison of BIRD kinetics for the same set of isomers was used in our previous investigation of the structure of singly hydrated clusters.[42] The inference of structure from relative kinetics rests on several assumptions. First, it is necessary to

**SCHEME 1**

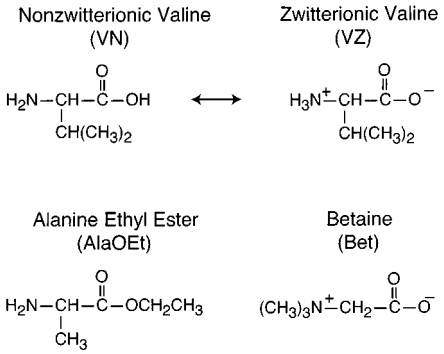


have good structural models for the two forms of valine; this requires that the interactions of the dissociating water molecule with the metal ion and the AA be the same in the valine and model clusters. Second, the activation and dissociation processes in the valine clusters must be comparable to those in the model clusters. In the BIRD experiment, this requires that integrated cross-sections for IR photon absorption and emission must be similar and that differences in dissociation entropy must be minimal or have no significant effect on the measured dissociation rate. In our previous study, we did extensive modeling to ensure that these requirements were fulfilled. In this report, we also include many theoretical results, in part to address these issues. With increasing cluster size, calculations become increasingly more difficult, not only because there are more atoms, but the number of possible conformers for each cluster increases dramatically. For the larger clusters, conducting an exhaustive search of the potential energy surface is not practical. Although we report dissociation kinetics for clusters of up to six water molecules, extensive theoretical efforts are confined to clusters with two and three water molecules. Limited theoretical results for the much larger Val·$Li^+(H_2O)_6$ cluster are also included due to its unusual stability measured experimentally.

The remainder of the results and discussion section is organized as follows. First, the stepwise hydration of the lithiated clusters is examined. Next, the sodiated clusters are considered, then the potassiated. Finally, results from numerical simulations of the experiments for $n = 2$ are presented in order to investigate the effects of differences in activation and dissociation processes on measured dissociation kinetics.

## M = Li

**AA·$Li^+(H_2O)_2$ Dissociation Kinetics.** Figure 1a shows blackbody dissociation kinetic data for AA·$Li^+(H_2O)_{2\rightarrow1}$ at 55 °C. Rate constants for the dissociation of the second water molecule from each cluster are determined from the slope of $\ln\{[AA{\cdot}Li^+(H_2O)_2]/([AA{\cdot}Li^+(H_2O)_2] + [AA{\cdot}Li^+(H_2O)_1] + [AA{\cdot}Li^+])\}$ vs time and are listed in Table 1. The data for all of the clusters from $n = 1-6$ can be fit by a straight line with $R^2$ values >0.99. The dissociation kinetics for AA = Val are virtually identical (within 3%) to those for AlaOEt, whereas water evaporates from the Bet cluster significantly (50%) more slowly. These dissociation kinetics clearly suggest that the second water is bound to the Val·$Li^+$ and AlaOEt·$Li^+$ clusters in a similar fashion and that this is different from the way it is bound to the Bet·$Li^+$ cluster; that is, the dissociation kinetics

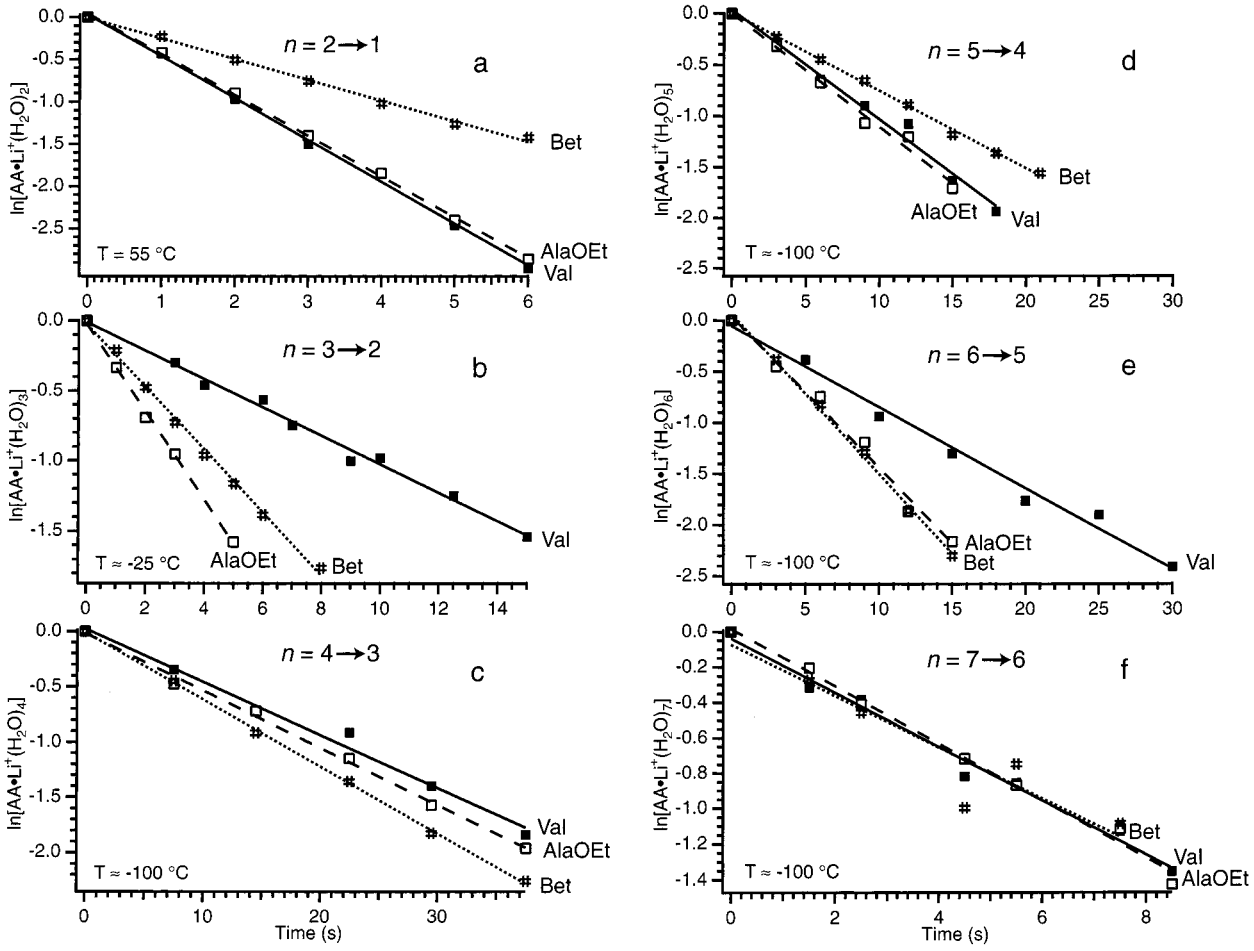


**Figure 1.** Blackbody infrared dissociation kinetics for the evaporation of water from AA·$Li^+(H_2O)_n$ clusters for $n = 2-7$.

**TABLE 1: Measured Dissociation Rates for $AA{\cdot}M^+(H_2O)_{n-n-1}$ and Percent Difference in Rates Referenced to the Isomeric Valine Cluster[a]**

| | | Li | | | Na | | | K | | |
|---|---|---|---|---|---|---|---|---|---|---|
| *n* | AA | *T* (°C) | rate ($s^{-1}$) | % diff. | *T* (°C) | rate ($s^{-1}$) | % diff. | *T* (°C) | rate ($s^{-1}$) | % diff. |
| 1 | Val | 108 | 0.0875 ± 0.0005 | | 25 | 0.0366 ± 0.001 | | −10 | 0.0476 ± 0.0009 | |
| | AlaOEt | 108 | 0.1000 ± 0.001 | +14% | 25 | 0.0339 ± 0.0007 | −7% | −10 | 0.0688 ± 0.0009 | +45% |
| | Bet | 108 | 0.1372 ± 0.002 | +57% | 25 | 0.0460 ± 0.0008 | +26% | −10 | 0.0510 ± 0.0006 | +7% |
| 2 | Val | 55 | 0.494 ± 0.01 | | 0 | 0.116 ± 0.003 | | −100 | 0.0091 ± 0.0002 | |
| | AlaOEt | 55 | 0.481 ± 0.01 | −3% | 0 | 0.140 ± 0.004 | +21% | −100 | 0.0113 ± 0.005 | +24% |
| | Bet | 55 | 0.245 ± 0.01 | −50% | 0 | 0.110 ± 0.003 | −5% | −100 | 0.0134 ± 0.001 | +47% |
| 3 | Val | −25 | 0.101 ± 0.003 | — | −25 | 0.187 ± 0.01 | — | −100 | 0.064 ± 0.002 | — |
| | AlaOEt | −25 | 0.314 ± 0.008 | +210% | −25 | 0.337 ± 0.02 | +80% | −100 | 0.069 ± 0.003 | +8% |
| | Bet | −25 | 0.224 ± 0.005 | +120% | −25 | 0.256 ± 0.01 | +37% | −100 | 0.082 ± 0.001 | +28% |
| 4 | Val | −100 | 0.048 ± 0.003 | | −100 | 0.048 ± 0.002 | | −150 | 0.0095 ± 0.0003 | — |
| | AlaOEt | −100 | 0.0517 ± 0.002 | +8% | −100 | 0.053 ± 0.003 | +10% | | 0.0095 ± 0.0002 | 0% |
| | Bet | −100 | 0.0607 ± 0.001 | +26% | −100 | 0.0496 ± 0.001 | +3% | | 0.0062 ± 0.0003 | −35% |
| 5 | Val | −100 | 0.107 ± 0.006 | | −100 | 0.113 ± 0.005 | | −150 | 0.028 ± 0.001 | — |
| | AlaOEt | −100 | 0.110 ± 0.006 | +3% | −100 | 0.092 ± 0.006 | −19% | | 0.040 ± 0.002 | +43% |
| | Bet | −100 | 0.0756 ± 0.001 | −29% | −100 | 0.081 ± 0.001 | −28% | | 0.0269 ± 0.0004 | −4% |
| 6 | Val | −100 | 0.079 ± 0.004 | | −100 | 0.112 ± 0.003 | | | | |
| | AlaOEt | −100 | 0.148 ± 0.008 | +87% | −100 | 0.200 ± 0.007 | +79% | | | |
| | Bet | −100 | 0.156 ± 0.004 | +97% | −100 | 0.184 ± 0.003 | +64% | | | |

[a] Error corresponds to the standard deviation of the linear least-squares best fit line to the first-order kinetic fit data.

suggest that Val is nonzwitterionic in this cluster. These kinetics primarily reflect differences in the binding energy of water. Although the kinetic data are extremely suggestive of structure, they are an indirect probe.

**$AA{\cdot}Li^+(H_2O)_2$ Low-Energy Structures.** Extensive modeling was done in order to identify low-energy conformations of $AA{\cdot}Li^+(H_2O)_2$ clusters as well as to ensure that AlaOEt and Bet are good models for the two forms of valine. A total of 54 conformers of $Val{\cdot}Li^+(H_2O)_2$ were optimized at the B3LYP/6-31G* level. Several of the structures selected from molecular dynamics minimized into the same conformer at this level of theory. Others minimized into structures that were presumably in equilibrium with each other, differing by the conformation of the side chain or position of the hydrogen bonds. To decrease the complexity of searching the entire potential energy surface, the lowest-energy structure within a group of similar conformations was selected as the representative structure for that group. From a few groups, two or more conformers were selected to check the reliability of this strategy.

The lowest-energy structure of each $AA{\cdot}Li^+(H_2O)_2$ isomer is illustrated in Figure 2. For VN, B3LYP and MP2 calculations predict different minimum-energy structures, both of which are shown in this figure. The nomenclature refers to *V*aline *N*onzwitterion (*V*aline *Z*witterion/*A*lanine ethyl ester/*B*etaine) with *2* waters, conformers *A*, *B*, *C*, etc. Conformer VN2_A is related to VZ2_A by the transfer of a proton, forming the zwitterion. The metal ion−water−AA interactions in VN2_B and A2_A appear to be virtually identical, indicating that A2_A is a good structural model for VN2_B. Likewise, B2_A is a good structural model for VZ2_A. B2_A also appears to be a good structural model for VN2_A.

MP2 and B3LYP calculations with the same large basis set predict different minimum-energy conformations. At the MP2/6-311++G** level of theory, VN2_B is the minimum-energy structure and is 2.4 kcal/mol lower in energy than the next lowest-energy conformer, VN2_A. In contrast, B3LYP calculations with the same basis set predict that VN2_A and VZ2_A are both somewhat (0.7−1.2 kcal/mol) more stable than VN2_B. Table 2 lists the relative energies of these candidate Val conformers at different levels of theory and calculated zero-point and thermal energy corrections. The energy differences among conformers are on the order of several kcal/mol, and the ordering of stability is not always constant at different levels of theory. This indicates that the calculations used here may not be adequate to determine the relative stability of these clusters. Thus, we use these theoretical results to guide our interpretation of the experimental data.

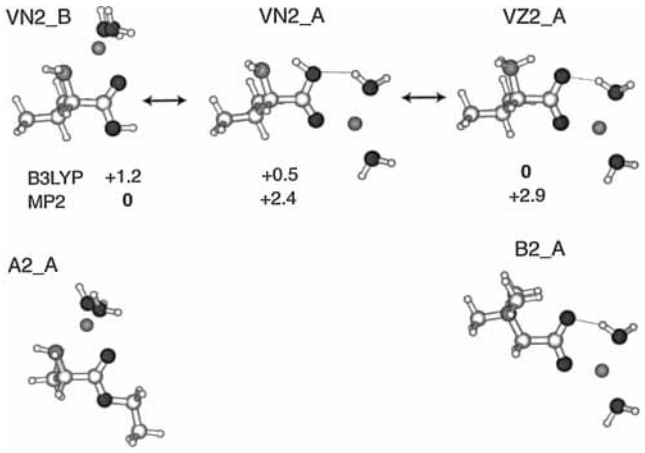


**Figure 2.** Lowest-energy structures for $AA{\cdot}Li^+(H_2O)_2$ complexes. The identity of the AA is labeled on the figure. Relative energies (in kcal/mol) for the AA = Val complexes are from single-point energy calculations at the B3LYP/6-311++G** level using the B3LYP/6-31+G*-optimized geometry and at the MP2/6-311++G** level using the MP2/6-31+G*-optimized geometry.

**TABLE 2: Relative Energies, in Kcal/Mol, of Selected $Val{\cdot}Li^+(H_2O)_2$ Conformations**

| method/basis | | VN2_A | VN2_B | VZ2_A |
|---|---|---|---|---|
| B3LYP/6-311++G*[a] | | 0.5 | 1.2 | 0 |
| MP2/6-31+G* | | 4.0 | 1.9 | 0 |
| 6-311++G**[a] | | 2.4 | 0 | 2.9 |
| RHF/6-31+G* | ΔZPE | 0 | 0 | 1.2 |
| | ΔG(55 °C) | 0 | 0.8 | 0.9 |
| Total B3LYP | | 0 | 1.6 | 1.5 |
| Total MP2 | | 1.5 | 0 | 4.1 |

[a] Single-point energy calculation at the 6-31+G* optimized geometry.

The experimental results are consistent with the structure of $Val{\cdot}Li^+(H_2O)_2$ being VN2_B, as predicted by the best MP2 calculations. If VN2_A or VZ2_A were the correct structure, the dissociation kinetics for $Val{\cdot}Li^+(H_2O)_2$ and $Bet{\cdot}Li^+(H_2O)_2$ should have been similar. Instead, these rates differ by ∼50%

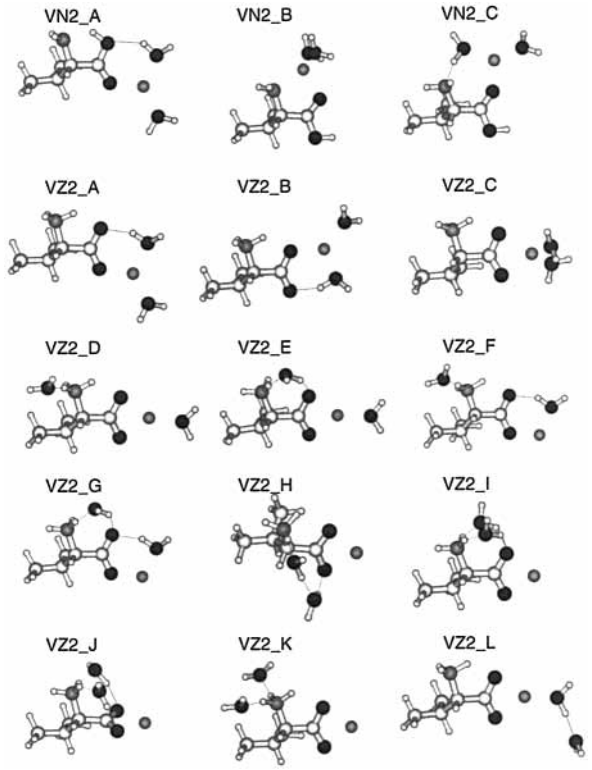


**Figure 3.** B3LYP/6-31G*-optimized structures for Val·$Li^+(H_2O)_2$ clusters. The relative energies of these structures are listed in Table 3.

(Figure 1, Table 1). Thus, the experimental results are not consistent with conformer VN2_A or VZ2_A. The slow dissociation rate measured for Bet·$Li^+(H_2O)_2$ compared to Val·$Li^+(H_2O)_2$ is also consistent with these structures because of the additional hydrogen bond binding the water molecule in conformer B2_A vs the purely electrostatic interaction in VN2_B.

**AA·$Li^+(H_2O)_2$ Additional Structures.** A more extensive selection of the Val·$Li^+(H_2O)_2$ conformers investigated is shown in Figure 3. The relative energies of these conformers for the lithiated clusters, as well as analogous clusters with M = Na and K, are listed in Table 3. Additional AlaOEt·$Li^+(H_2O)_2$ and Bet·$Li^+(H_2O)_2$ conformers are shown in Figure 4. The water molecules in all of these low-energy structures are coordinated to charged sites. For the VN and AlaOEt structures, this is the metal ion. For VZ and Bet structures, the second water may coordinate to the metal ion, to the carboxylate group, or to the protonated N terminus of the valine or the much more diffuse charge of the quaternary amine of the betaine.

Comparing the valine clusters in Figure 3 to the model clusters in Figure 4, it is apparent that AlaOEt and Bet provide good structural models for all of the energetically competitive lithiated Val conformers. Clusters in which nonzwitterionic valine coordinates the metal ion between the nitrogen and carbonyl oxygen, VN2_B and VN2_C, are well mimicked by the AlaOEt clusters A2_A and A2_B, respectively. Clusters in which the metal ion coordinates to the C terminus of valine, VN2_A and VZ2_A−C, are well modeled by B2_A−C.

Val conformers for which AlaOEt and Bet do not provide good structural models are VZ2_D−K. In all of these conformers, water hydrogen bonds to the protonated amine of valine, a functionality that is not present in any of the model clusters. For the lithiated clusters, VZ2_D−K are significantly (8−22 kcal/mol) higher in energy than the minimum-energy structure. For this reason, we do not believe that these are viable structures. They are included here to illustrate the variety of structures that were examined. As the size of the metal ion increases, some of these structures become more energetically competitive. This will be discussed later.

*Overall, the addition of a second water molecule does not appear to significantly affect the structure of the Val·$Li^+$ complex.* In the complex with no water molecules, lithium is coordinated between the nitrogen and carbonyl oxygen of nonzwitterionic valine. A single water molecule coordinates to this complex through an interaction with just the metal ion.[42] In VN2_B, the conformation indicated by the combined theoretical and experimental results, the second water molecule also coordinates only to the metal ion. Calculations indicate that these two water molecules do not help stabilize the zwitterionic form of valine (i.e., VZ2_A) relative to the NO-coordinated nonzwitterionic form. In our previous work, we found that the nonhydrated nonzwitterionic complex is 3.3 kcal/mol more stable than the zwitterionic complex. Here, the difference is calculated to be 2.9 kcal/mol at the same level of theory. Perhaps this is not surprising, as the water molecules' only direct interactions are with the metal ion itself and not with the amino acid.

**AA·$Li^+(H_2O)_3$ Dissociation Kinetics.** Kinetics for evaporation of water from AA·$Li^+(H_2O)_3$ clusters at a nominal temperature of −25 °C are shown in Figure 1b, and the dissociation rates are listed in Table 1. The kinetics for the loss of the third water molecule are dramatically different from those for the loss of the second water molecule (Figure 1a). Val·$Li^+(H_2O)_3$ dissociates at less than one-half the rate of the Bet·$Li^+(H_2O)_3$ and less than one-third the rate of the AlaOEt·$Li^+(H_2O)_3$, indicating that this cluster does not resemble either of the model clusters.

**AA·$Li^+(H_2O)_3$ Low-Energy Structures.** Figure 5 shows the most likely low-energy structures for AA·$Li^+(H_2O)_3$. At the B3LYP/6-311++G** level of theory, VN3_A and VZ3_B are the lowest-energy structures and are nearly degenerate. At the MP2/6-311++G** level, VN3_A and VN3_F are the lowest-energy structures and are nearly degenerate. The energy differences between these conformers are relatively small and fluctuate with the level of theory used. Therefore, it is not possible to determine the lowest-energy conformer based on these calculations alone.

It is possible to discriminate among the candidate valine structures in Figure 5 based on the experimental data. A3_A is a good model for VN3_F, but the measured dissociation rates of AlaOEt·$Li^+(H_2O)_3$ and Val·$Li^+(H_2O)_3$ differ by a factor of 3, indicating that VN3_F is not the conformation of the valine cluster. Similarly, if VN3_A were the correct structure of Val·$Li^+(H_2O)_3$, the dissociation rate measured for the valine and betaine cluster should be similar. Instead, the betaine cluster dissociates more than twice as fast as the valine cluster (Table 1). This strongly suggests that VN3_A is not the conformation of Val·$Li^+(H_2O)_3$. In VZ3_B, one of the waters forms a hydrogen bond with the protonated amine of valine. Neither AlaOEt nor Bet has a protonated amine. The bulky methyl groups surrounding the N terminus of betaine will not form hydrogen bonds that are nearly as strong as those in the valine complex. Thus, the binding of this water molecule in VZ3_B does not resemble that in of either of the model clusters. Hence, of the three valine clusters illustrated in Figure 5, conformer VZ3_B is the only one consistent with the experimental data.

**AA·$Li^+(H_2O)_3$ Additional Structures.** Although we believe VZ3_B is the best candidate for the lowest-energy conformation of Val·$Li^+(H_2O)_3$, there are several other possible conforma-

**TABLE 3: Relative Energies, in kcal/mol, of Selected Val·$M^+(H_2O)_2$ Conformations Illustrated in Figure 3, Calculated Using the B3LYP Method with Basis Sets of Increasing Size**

| | VN conformers | | | VZ conformers | | | | | | | | | | | |
|---|---|---|---|---|---|---|---|---|---|---|---|---|---|---|---|
| M: basis set | A | B | C | A | B | C | D | E | F | G | H | I | J | K | L |
| Li: 6-31G* | 2.1 | 0.8 | 3.2 | 0 | 3.8 | 2.5 | 7.9 | 8.2 | 9.3 | 10.0 | 20.2 | 22.2 | 23.5 | 22.9 | 9.0 |
| 6-31+G* | 2.8 | 3.3 | 4.6 | 0 | *b* | 2.4 | 6.4 | 7.5 | | | | | | | |
| 6-311++G**[a] | 0.5 | 1.2 | 2.5 | 0 | *b* | | 6.9 | 8.1 | | | | | | | |
| Na: 6-31G* | 0.5 | 1.6 | 1.9 | 0 | 2.5 | 2.1 | 4.5 | 4.5 | 4.8 | | 9.4 | 12.0 | 13.1 | | |
| 6-31+G* | 1.5 | 4.2 | 3.3 | 0 | *b* | | 3.8 | 5.5 | | | | | | | |
| 6-311++G**[a] | 0 | 2.8 | 2.5 | 0.8 | *b* | | 4.7 | 5.4 | | | | | | | |
| K: LACVP* | 0 | 3.9 | 1.8 | 1.9 | *b* | 3.5 | 4.4 | 4.3 | 1.8 | 1.7 | 2.1 | 4.7 | 5.7 | 7.5 | 4.8 |
| LACVP+* | 0.8 | 8.6 | 2.6 | 1.2 | *b* | | | | 0 | 1.3 | 2.4 | 5.4 | 7.0 | | |
| LACVP++**[a] | 0 | 7.4 | 1.9 | 2.0 | *b* | | | | 1.3 | 2.8 | 4.1 | 7.0 | 8.8 | | |

[a] Single-point energy calculation. [b] Conformation not stable at this level of theory.

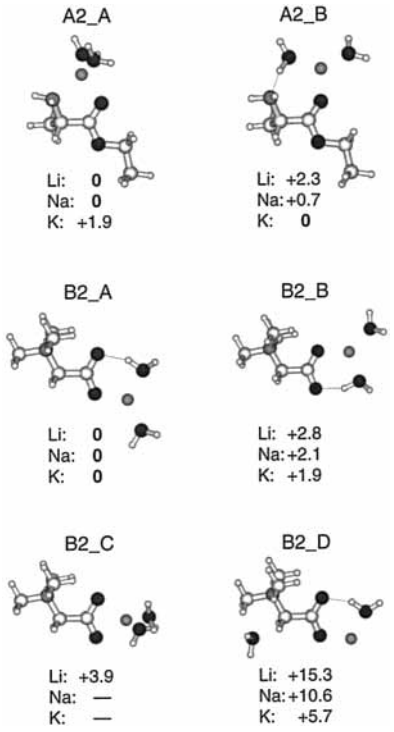


**Figure 4.** B3LYP/6-31G*-optimized structures and relative energies (in kcal/mol) for AlaOEt·$Li^+(H_2O)_2$ and Bet·$Li^+(H_2O)_2$ clusters.

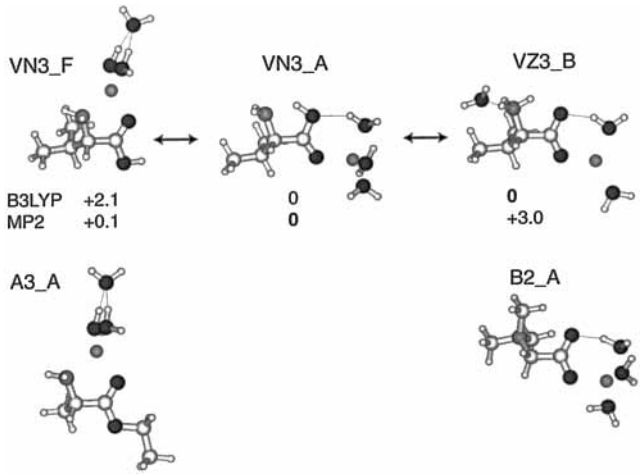


**Figure 5.** Lowest-energy structures for AA·$Li^+(H_2O)_3$ complexes. The identity of the AA is labeled on the figure. Relative energies (in kcal/mol) for the AA = Val complexes are from single-point energy calculations at the B3LYP/6-311++G** level using the B3LYP/6-31+G*-optimized geometry and at the MP2/6-311++G** level using the MP2/6-31+G*-optimized geometry.

tions. A total of 49 structures of Val·$Li^+(H_2O)_3$ were optimized at the B3LYP/6-31G* level. Twelve of these are shown in Figure 6. The relative energies of six of these structures at several levels of theory are listed in Table 4. Three structures each of AlaOEt·$Li^+(H_2O)_3$ and Bet·$Li^+(H_2O)_3$ are shown in Figure 7. There are many more energetically competitive conformers for the trihydrated clusters than there are for the dihydrates. With the exception of VZ3_D, all of the conformers shown in Figure 6 are relatively close in energy, within 2.6 kcal/mol, at the B3LYP/6-311++G** level. Therefore, these conformers cannot be discounted on the basis of their calculated energies alone. Several of these conformers are inconsistent with the experimental results and can be ruled out. The AA-Li−$H_2O$ interactions in valine cluster conformations in which the metal is bound to the C-terminus of valine (e.g., VN3_A−D, VZ3_A) are well modeled by betaine clusters. Similarly, conformations in which the metal is coordinated between the nitrogen and carbonyl oxygen of nonzwitterionic valine (e.g., VN3_E−G) are well modeled by the AlaOEt clusters. Clusters for which there are not good model structures, and which therefore cannot be ruled out based on experimental results, are VN3_H and VZ3_B−D. As discussed before, VZ3_B is the lowest-energy structure and therefore, we believe, the most likely candidate. VZ3_D is extremely unlikely based on its significantly higher (+7.5 kcal/mol) energy. VN3_H is the only candidate VN conformer. However, it is 2.6 kcal/mol higher in energy than the minimum energy structures and, therefore, seems less likely to be the lowest-energy structure.

It should be emphasized that these experiments probe differences between the populated bound structure(s) and the transition state(s) for dissociation. Under the conditions of the experiment, more than one conformer is likely to be present, and some of these conformers likely interconvert. For example, nonzwitterion structure VN3_A and the zwitterion structure VZ3_A differ only by the position of the acidic proton. The barrier for proton transfer is likely to be very low. In contrast, conversion of either of these structure to zwitterion VZ3_B requires transfer of one water molecule from the lithium ion at the C-terminal end of the valine to the protonated N-terminal nitrogen. The barrier for this transfer should be substantial. Although these structures could conceivably interconvert in these experiments, the measured kinetics should depend most strongly on the most populated (lowest-energy) structure. Therefore, we believe that the measured dissociation kinetics can probe these relatively subtle differences in structure.

Overall, the combined experimental and theoretical results strongly suggest that the valine in Val·$Li^+(H_2O)_3$ has a zwitterionic form. The third water of the cluster appears to be the first water molecule which hydrogen bonds to the valine and *does not* interact directly with the metal ion. *This third water molecule changes the mode of metal ion binding from NO*

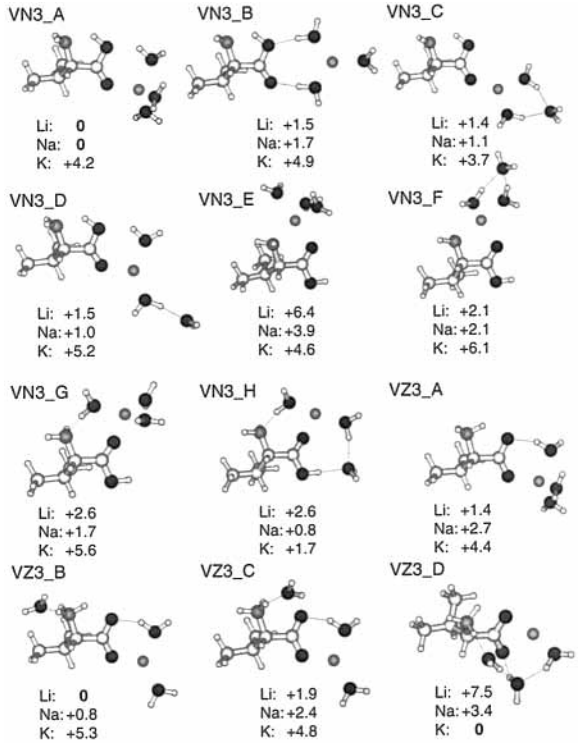


**Figure 6.** B3LYP/6-31G*-optimized structures of Val·$Li^+(H_2O)_3$ clusters. Relative energies (in kcal/mol) are indicated at the B3LYP/6-311++G** level for M = Li and Na and at the B3LYP/LACVP* level for M = K.

*coordination to OO coordination. Moreover, this third water molecule appears to stabilize the charge separation of the zwitterion sufficiently to cause the proton-transfer to occur, resulting in the transformation of valine into its solution-phase conformation.*

**AA·$Li^+(H_2O)_n$, $n$ = 4−7: Dissociation Kinetics.** The relative dissociation kinetics for AA·$Li^+(H_2O)_n$ clusters, $n$ = 4−7 are shown in Figure 1c−f. All of these data were measured at a very low nominal temperature, −100 °C. Attaining sufficient ion signal to measure kinetics for $n$ = 7 is difficult, so there is significant scatter in the kinetics shown in Figure 1f. For $n$ = 4 and 5, the dissociation rates of both of the model clusters are within 30% of the Val cluster, with AlaOEt being the closer of the two. There is no obvious interpretation of this kinetic data in terms of structure. It is somewhat surprising that the fifth water molecule dissociates more quickly from the valine cluster than from the Bet cluster. It seems unlikely that, with three waters, lithiated valine adopts a zwitterionic structure but goes back to nonzwitterionic form with four and five waters, although this is a possible interpretation of the $n$ = 4 and 5 kinetic data. A more probable explanation is that AlaOEt and Bet are not good models for the clusters of higher extents of hydration and that the binding of the fourth and fifth water molecules in all of these clusters is extremely weak. The similar relative kinetics are due to similar weak binding interactions (i.e., primarily hydrogen bonding interactions) in all of the clusters and reflect slight differences in cluster photoactivation rates. Likewise, the fast dissociation and similarity of the measured dissociation rates for all three $n$ = 7 clusters (Figure 1f) suggests the binding of water to these clusters is weak and probably nonspecific.

The kinetics for the loss of the fifth and sixth water molecules (Figure 1d−e) were measured at the same nominal temperature and have been plotted with the same scale. The dissociation rates are listed in Table 1. Remarkably, the rate for the dissociation of the sixth water molecule from the valine cluster is slower than that of the fifth! This is not the case for the AlaOEt and Bet clusters. For both of these clusters, as well as for all clusters of lower hydration, the dissociation of the ($n$ + 1)th water molecule is faster than that of the $n$th when measured at the same temperature. Presumably, this is due to the stronger binding of the $n$th water molecule compared to the ($n$ + 1)th water, although it is also true that the larger cluster will absorb photons and become activated faster than the smaller cluster. The fact that the sixth water molecule is slower to dissociate from the valine cluster than the fifth indicates that Val·$M^+$-$(H_2O)_6$ is unusually stable relative to Val·$M^+(H_2O)_5$.

**AA·$Li^+(H_2O)_6$: Structures.** To further investigate this surprising phenomenon, several possible structures of Val·$Li^+$-$(H_2O)_6$ were examined. These are shown in Figure 8. Unlike the conformations for the doubly and triply hydrated clusters, the hexahydrated conformers shown are not derived from an extensive search of the potential energy surface for this cluster. Instead, a limited number of structures were examined and the representative lowest-energy structures are shown in Figure 8. All of the low-energy clusters exhibit extensive hydrogen bonding. The zwitterionic valine complex has three charge sites available for hydrogen bonding vs only one in the nonzwitterionic complex. In all of the low-energy conformers of the VZ complex, all six water molecules coordinate directly to charge sites, and the lithium ion is tetrahedrally coordinated by a combination of water molecules and heteroatoms of the valine. According to high-level calculations, tetrahedral coordination is the preferred coordination geometry of lithium−water clusters.[46,47] In the VN structures, the lithium is pentacoordinate, and two or three of the water molecules are not coordinated to charge sites. This indicates that water binding to the VN structures will be weaker than that to the VZ structures and suggests that the VZ clusters will be more stable. However, this does not explain the special stability of Val·$Li^+(H_2O)_6$ vs Val·$Li^+(H_2O)_5$.

One possible explanation is that, with five waters, the valine in the lithiated cluster is nonzwitterionic and that the conformation changes to zwitterionic with the inclusion of a sixth water molecule. As indicated above, water should bind more strongly to the zwitterionic complex, which would explain the slower dissociation of the sixth vs the fifth water molecule. However, because of the strong evidence for the zwitterionic form of valine in the trihydrated cluster, we do not believe that this is the most likely explanation. An alternative, and we believe more probable, explanation is that the conformation of the valine in the Val·$Li^+(H_2O)_5$ cluster is somewhat strained compared to that of valine in clusters with four and six water molecules. This would decrease the binding energy of the fifth water molecule. A scenario describing this is detailed below for VZ6_A, the most stable cluster conformation identified.

On Figure 8, we have numbered the water molecules by probable order of attachment to VZ6_A. Water molecules 1, 2, and 3 are basically the same as the three water molecules in VZ3_B (Figures 5 and 6), the most likely candidate for the structure of the Val·$Li^+(H_2O)_3$ cluster. Position 4 is probably the next most stable water-binding site based on lithium's ability to comfortably accommodate four ligands and on the similar energies computed for conformers VZ3_A and VZ3_B (Figure 6). The fifth water molecule would likely bridge between the N and C termini of the valine, forming two hydrogen bonds at the expense of a small distortion in the backbone of the valine, the C terminal end of which is rotated from its most favorable position. Thus, the valine in the cluster with five waters is somewhat strained in order to form the maximum number of

**TABLE 4: Relative Energies, in kcal/mol, of the Most Competitive Val·Li$^+$(H$_2$O)$_3$ Conformers**

| method/basis | VN3__A | VN3__F | VN3__H | VZ3__A | VZ3__B | VZ3__C |
|---|---|---|---|---|---|---|
| B3LYP/6-31G* | 0.6 | 1.7 | 2.9 | 0 | 2.8 | 2.7 |
| 6-31+G* | 1.9 | 3.8 | 4.0 | 0.8 | 0 | 1.4 |
| 6-311++G** [a] | 0 | 2.1 | 2.6 | 1.4 | 0 | 1.9 |
| MP2/6-31G* | 2.6 | 1.8 | 4.2 | 0.3 | 0.3 | 0 |
| 6-311++G** [a] | 0 | 0.1 | 3.6 | 2.2 | 3.0 | 3.1 |

[a] Single-point energy calculation at 6-31+G*-geometry optimized structure.

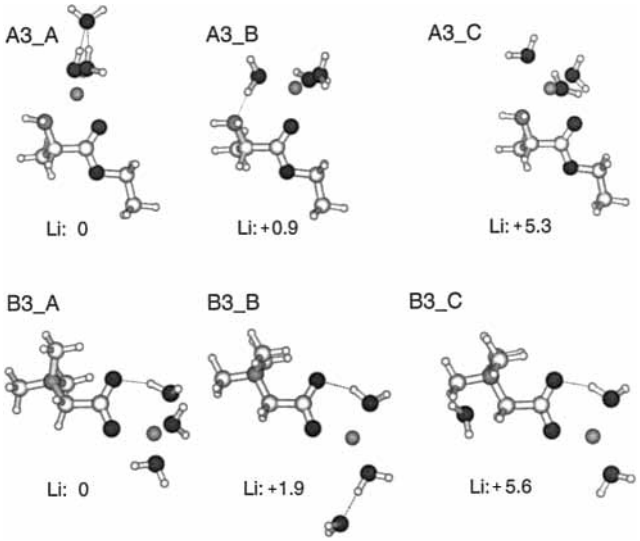


**Figure 7.** B3LYP/6-31G*-optimized structures and relative energies (in kcal/mol) for AlaOEt·Li$^+$(H$_2$O)$_3$ and Bet·Li$^+$(H$_2$O)$_3$ clusters.

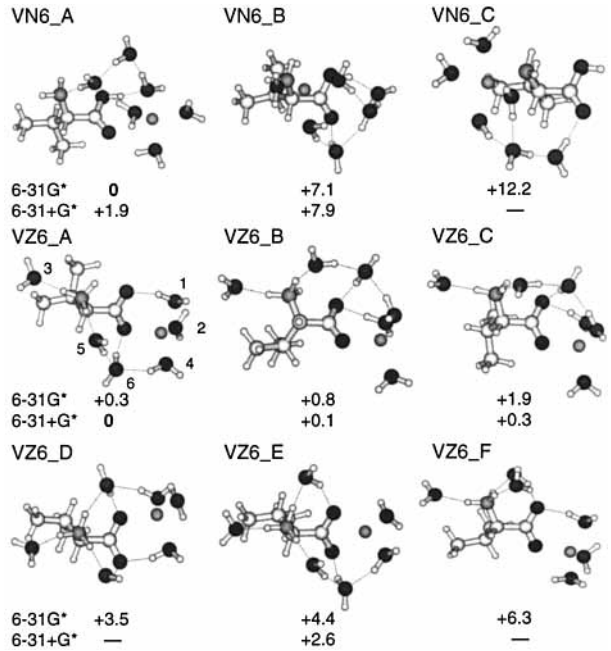


**Figure 8.** B3LYP/6-31G*-optimized structures for Val·M$^+$(H$_2$O)$_6$ clusters with relative energies (in kcal/mol) from B3LYP/6-31G* and B3LYP/6-31+G* optimization. Proposed ordering of water molecule attachment is noted for VZ6__A.

hydrogen bonds. Water molecule 6 breaks one of those hydrogen bonds but forms three new H bonds, relieving the valine backbone strain. Interestingly, the coordination geometry of waters 4, 5, and 6 form a stable three-member group of hydration as seen in conformer VZ3__D (Figure 6). This scenario is consistent with the measured kinetics for the $n = 5$ and 6 clusters. Although the conformer VZ6__A and scenario above can explain the unusual dissociation kinetics of the Val·M$^+$(H$_2$O)$_5$ and Val·M$^+$(H$_2$O)$_6$ clusters, it is only one of a number of possible explanations. What is certain is that something unusual happens at this extent of hydration.

## M = Na

**AA·Na$^+$(H$_2$O)$_2$ Dissociation Kinetics.** Figure 9 shows the dissociation kinetics for AA·Na$^+$(H$_2$O)$_n$ clusters, $n = 2-6$. The dissociation rates for these clusters are listed in Table 1. The difference in the rate of dissociation for the second water molecule between the AA·Na$^+$(H$_2$O)$_2$ clusters is much smaller than it is for the AA·Li$^+$(H$_2$O)$_2$ clusters. At 55 °C, all three clusters dissociate with virtually the same rate (data not shown). However, at a nominal temperature of 0 °C, the kinetic data indicate that the dissociation of the second water molecule from Val·Na$^+$(H$_2$O)$_2$ resembles that from Bet·Na$^+$(H$_2$O)$_2$, whereas the second water molecule dissociates from AlaOEt·Na$^+$(H$_2$O)$_2$ somewhat (~20%) faster (Figure 9a and Table 1). The lower-temperature data suggest that the sodiated valine cluster with two waters closely resembles the Bet cluster, not the AlaOEt cluster. Furthermore, the faster dissociation rate of the second water molecule from the sodiated clusters than from the lithiated clusters suggests that the second water is bound more weakly to the sodiated clusters than to the lithiated ones.

**AA·Na$^+$(H$_2$O)$_2$ Structures.** Conformers of AA·Na$^+$(H$_2$O)$_2$ were manufactured from the set of AA·Li$^+$(H$_2$O)$_2$ cluster conformations, the most important of which are illustrated in Figures 3 and 4. The relative energies for the sodiated clusters are listed in Table 3. B3LYP/6-311++G** calculations indicate that the OO-coordinated valine conformers VN2__A and VZ2__A are the most stable cluster structures. Because the dissociation of water from both VN2__A and VZ2__A is likely to be well modeled by the betaine cluster B2__A, the experiment cannot distinguish between these structures. Both of these conformers are consistent with experimental results suggesting that the sodium and waters are coordinated to the C terminus of valine in Val·Na$^+$(H$_2$O)$_2$ clusters. At the highest level of theory, VN2__A is marginally (0.8 kcal/mol) more stable than VZ2__A. Zero-point energy and thermal energy corrections increase this difference to 3 kcal/mol (Table 5). In the Li$^+$ cluster calculations, MP2 theory stabilizes the VN clusters relative to the VZ clusters, and it is likely that a similar effect would occur in the sodiated clusters. Thus, calculations indicate that VN2__A is the most stable conformation of Val·Na$^+$(H$_2$O)$_2$.

In VN2__A, the conformation indicated for Val·Na$^+$(H$_2$O)$_2$, the sodium ion is coordinated to the C terminus of the valine. In the singly hydrated sodium cluster, the metal is coordinated between the N and C termini of the valine. If this were the case for the doubly hydrated sodium clusters, the dissociation kinetics for Val·Na$^+$(H$_2$O)$_2$ should have been similar to those of AlaOEt·Na$^+$(H$_2$O)$_2$. *Both the similar dissociation rate to Bet·Na$^+$(H$_2$O)$_2$ and the calculated lowest-energy conformation indicate that the addition of the second water molecule has altered the preferred binding site of the metal ion in this cluster*. This is in contrast to the lithiated cluster results, which indicated that the second water molecule had little apparent effect on the mode of metal ion binding.

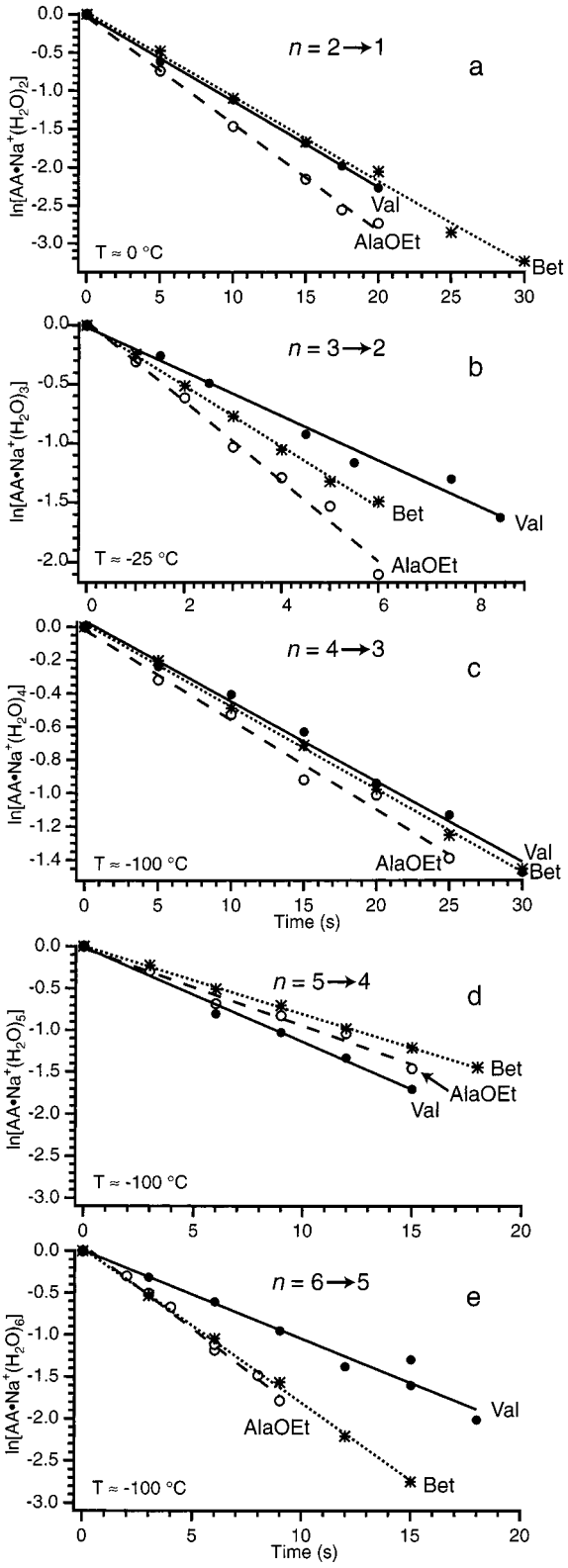


**Figure 9.** Blackbody infrared dissociation kinetics for the evaporation of water from $AA{\cdot}Na^+(H_2O)_n$ clusters for $n = 2-6$.

**$AA{\cdot}Na^+(H_2O)_3$ Dissociation Kinetics.** The dissociation kinetics for $AA{\cdot}Na^+(H_2O)_3$ are shown in Figure 9b. These kinetics were measured at the same nominal temperature as those for the loss of the third water from the lithiated clusters, −25 °C. Qualitatively, the kinetics are similar to the lithium data, although the sodiated clusters are somewhat faster to dissociate, and the rate spread between isomers is not as great. The third water molecule dissociates much more slowly from the Val cluster than from either the AlaOEt or Bet cluster. These data indicate that the third water molecule binds differently to $Val{\cdot}Na^+$ than it does to clusters of either of the model compounds.

**$AA{\cdot}Na^+(H_2O)_3$ Structures.** The same set of conformers investigated for $AA{\cdot}Li^+(H_2O)_3$ (Figures 6 and 7) was used to study the structure of the sodiated clusters. For $Val{\cdot}Na^+(H_2O)_3$, the lowest-energy conformer is VN3_A (Figure 6). However, there are many conformers of similar energy. Conformers VN3_D, VN3_H, and VZ3_B are all within 1 kcal/mol of VN3_A, and several more conformers are within 2 kcal/mol. It is unlikely that VN3_A is the conformation of $Val{\cdot}Na^+(H_2O)_3$ because the dissociation kinetics for this cluster are so different from those of the betaine cluster. The measured relative kinetics can also be used to discount other conformers. All of the VN clusters that have the metal ion at the C-terminal end of valine (VN3_A−D) resemble Bet clusters. All of the NO-coordinated VN clusters (VN3_E−G) have AlaOEt cluster analogues. The only VN conformer identified that does not resemble any of the model clusters is VN3_H. This is a possible structure for $Val{\cdot}Na^+(H_2O)_3$ and is calculated to be within 0.8 kcal/mol of the minimum. Among the VZ clusters, VZ3_A can be ruled out because of its similarity to B3_A. VZ3_B−D are all possible conformations for $Val{\cdot}Na^+(H_2O)_3$. Among these, VZ3_B is the most likely based on its lower energy. Thus, for M = Na, it is unclear whether the valine adopts a nonzwitterionic form, VN2_H, or a zwitterionic form such as VZ3_B.

**$AA{\cdot}Na^+(H_2O)_n$, $n = 4-6$, Dissociation Kinetics.** The dissociation kinetics for $AA{\cdot}Na^+(H_2O)_n$, $n = 4-6$, measured at a nominal temperature of −100 °C, are shown in Figure 9c−e. For $n = 4$, the rate of dissociation for both of the model clusters is within 10% of the valine cluster. For $n = 5$, this difference is somewhat larger. As was the case for the lithiated clusters of the same extents of hydration, there is no obvious structural interpretation for these data. It is doubtful that AlaOEt and Bet are adequate structural models for either of the two forms of valine with this number of water molecules present. The similarity in rates can be explained by the similarly weak water-binding interactions present in all of the clusters.

The dissociation of the sixth water molecule from the sodiated valine cluster is slower than that of the fifth; the same phenomenon that was observed for the lithiated clusters. Again, these results indicate that the sixth water molecule is especially stable relative to the fifth. Calculations have not been done on sodiated clusters with $n = 6$, but we speculate that this cluster has a zwitterionic conformation similar to that of $AA{\cdot}Li^+(H_2O)_6$ based on the special stability of these clusters.

## M = K

**Dissociation Kinetics.** Dissociation kinetics for $AA{\cdot}K^+(H_2O)_n$, $n = 2-5$ are shown in Figure 10. The ion signal was insufficient to measure the kinetics for $n = 6$. Dissociation of the $n$th water molecule from the potassiated clusters is much faster than that from the lithiated or sodiated clusters at the same nominal temperature. The dissociation data shown in Figure 10 was measured at very cold nominal temperatures (−100 to −150 °C). The dissociation rates are given in Table 1.

**$AA{\cdot}K^+(H_2O)_2$.** At −100 °C, the second water is slower to dissociate from the valine cluster than from either of the model clusters. The difference in rates is only moderate for the AOEt cluster (24% difference in rate) and much larger (47% difference) for the Bet cluster. These data suggest that the valine cluster does not resemble either of the potassiated model clusters.

Interpretation of the potassiated data is difficult because the water molecule binding sites involve relatively weak interac-

**TABLE 5: Relative Energies, in kcal/mol, of the Most Competitive Val·$Na^+(H_2O)_2$ Conformers**

| method/basis | | VN2_A | VN2_B | VN2_C | VZ2_A | VZ2_D |
|---|---|---|---|---|---|---|
| B3LYP/6-311++G**[a] | | 0 | 0.6 | 2.5 | 0.8 | 4.7 |
| RHF/6-31+G* | ΔZPE | 0 | −0.3 | 0.5 | 1.2 | 0.6 |
| | Δ*G*(0 °C) | 0 | 1.5 | 0.8 | 0.9 | −0.2 |
| | Δ*G*(55 °C) | 0 | 1.9 | 1.0 | 1.1 | −0.3 |
| total B3LYP (0 °C) | | 0 | 1.8 | 3.8 | 3.0 | 5.0 |
| total B3LYP (55 °C) | | 0 | 2.2 | 4.0 | 3.2 | 4.9 |

[a] Single-point energy calculation at B3LYP/6-31+G* geometry optimized structure.

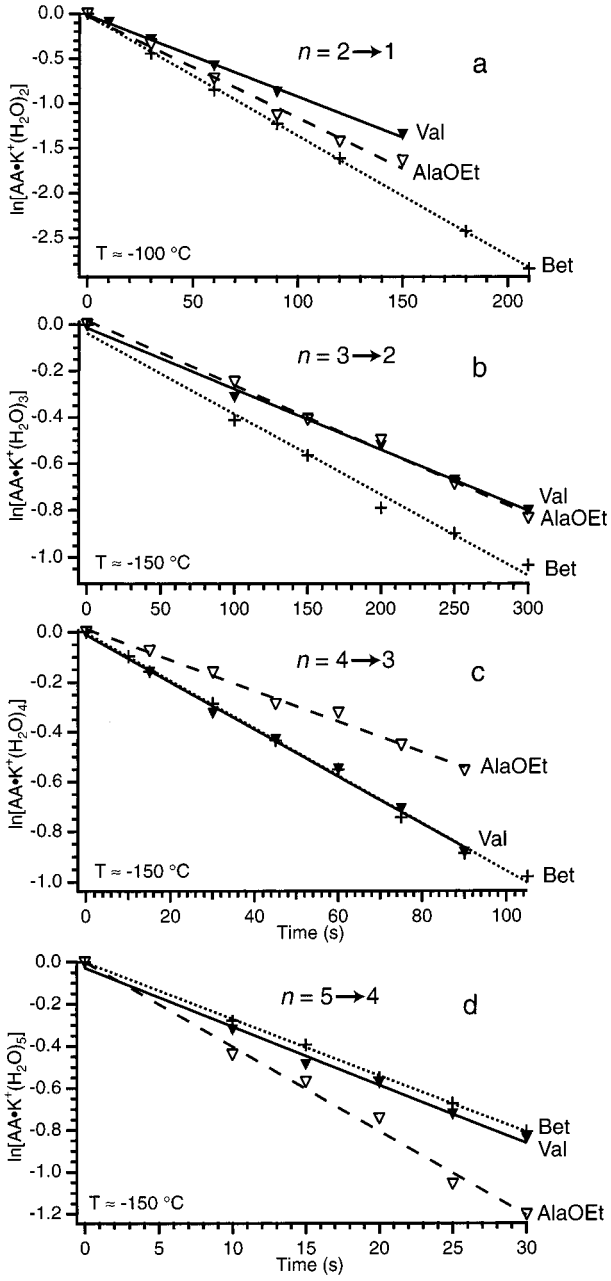


**Figure 10.** Blackbody infrared dissociation kinetics for the evaporation of water from AA·$K^+(H_2O)_n$ clusters for $n = 2-5$.

tions: hydrogen bonds or coordination to the very diffuse positive charge of the potassium ion. The weak binding energy of water molecules to all of the potassiated clusters means that small changes in the binding energy make larger differences in the observed dissociation rates than is the case for more strongly bound clusters. It is possible or even likely that the relative kinetics are no longer a good probe of structure for these clusters. This occurs at lower hydration number in the potassiated clusters than the lithiated or sodiated due to the weaker binding of water in these clusters.

The same set of conformers of dihydrated clusters, illustrated in Figures 3 and 4 for M = Li, were considered for M = K. Table 6 lists the energies of the five most likely of these conformers, including zero-point and thermal energy corrections. The lowest-energy structure at the B3LYP/LACVP++** level of theory is VN2_A. In this conformer, the metal ion is bound to the C terminus of nonzwitterionic valine, and it is the most likely structure of Val·$Na^+(H_2O)_2$. If VN2_A is the correct structure of the potassiated cluster, then Val·$K^+(H_2O)_2$ should dissociate with approximately the same rate as Bet·$K^+(H_2O)_2$. However, the dissociation of the betaine cluster is approximately 50% faster than the Val cluster at −100 °C (Table 1). This suggests that VN2_A is not the correct structure of Val·$K^+$-$(H_2O)_2$, although we cannot entirely discount the possibility that the binding energy of water to the nonzwitterionic valine cluster is slightly different from the binding energy of water to the (zwitterionic) betaine cluster. An explanation more consistent with experimental results is that the structure of the valine cluster does not resemble either of the model clusters. Of the conformers we examined, VZ2_F is the most likely candidate based on its calculated energy. However, calculated zero-point and thermal energy corrections (Table 6) significantly destabilize this conformer with respect to the minimum-energy conformer.

**AA·$K^+(H_2O)_3$.** For $n = 3$, the dissociation kinetics measured for the potassiated clusters do not show the dramatic differences in rates measured for the clusters containing lithium and sodium. Instead, the Val and AlaOEt clusters dissociate at approximately the same rate, and the Bet cluster dissociates somewhat (∼25%) faster. As with the AA·$K^+(H_2O)_2$ clusters, these dissociation kinetics were measured at a very cold nominal temperature, −150 °C, indicating that the binding is extremely weak. One possible interpretation of the kinetic data is that the metal ion and water binding in Val·$K^+(H_2O)_3$ resembles that in AlaOEt·$K^+(H_2O)_3$. However, because the dissociation kinetics of the second water suggested that the valine cluster is not modeled well by either AlaOEt or Bet, this seems unlikely. Rather, it is more probable that the clusters have different structures which have similar, weak water-binding energies.

Among the structures illustrated in Figure 6, the lowest-energy conformer of Val·$K^+(H_2O)_3$ is VZ3_D. The only structure within 3.5 kcal/mol of VZ3_D is VN3_H. Neither of these conformers is well modeled by Bet or AlaOEt clusters, despite the similarity of the Val·$K^+(H_2O)_3$ and AlaOEt·$K^+(H_2O)_3$ kinetics. This underscores the likelihood that clusters which do not resemble each other structurally may have similar dissociation kinetics when the binding energy is so weak.

**AA·$K^+(H_2O)_n$, $n = 4-5$.** The dissociation rate for the fourth and fifth water molecules from Val·$K^+$ clusters is approximately the same as that from the Bet·$K^+$ clusters and moderately different from the AlaOEt·$K^+$ clusters. Again, we do not believe that the similarity in measured dissociation rates reflects a similarity in structure. Rather, the relative kinetics are no longer a good probe of structure due to the lack of good models for

**TABLE 6: Relative Energies, in kcal/mol, of Most Competitive Val·K$^+$(H$_2$O)$_2$ Conformations**

| method/basis set | | VN2_A | VN2_C | VZ2_A | VZ2_F | VZ2_H |
|---|---|---|---|---|---|---|
| B3LYP/LACVP++**[a] | | 0 | 1.9 | 2.0 | 1.3 | 4.1 |
| RHF/LACVP+* | $\Delta$ZPE | 0 | 0.5 | 1.1 | 1.7 | 2.5 |
| | $\Delta G$(−100 °C) | 0 | −0.3 | −0.5 | 0.1 | 0.9 |
| total B3LYP (−100 °C) | | 0 | 2.1 | 2.6 | 3.1 | 7.5 |

[a] Single-point energy calculation at B3LYP/LACVP+* geometry optimized structure.

**TABLE 7: Effect of Transition State Entropy on Modeled Dissociation Rates for Val·M$^+$(H$_2$O)$_2$**

| M | $T$ (°C) | model $E_0$ (kcal/mol) | "neutral" TS Rate (s$^{-1}$) | "loose" TS Rate (s$^{-1}$) |
|---|---|---|---|---|
| Li | 55 | 16.0 | 0.427 | 0.686 |
| Na | 0 | 12.5 | 0.106 | 0.127 |
| K | −100 | 7.5 | 0.0071 | 0.0074 |

clusters of higher hydration state and the weakness of water binding to all of these clusters.

### AA·M$^+$(H$_2$O)$_2$: Master Equation Analysis

Numerical simulations of the BIRD experiment provide insight into the relative effects of differences in activation processes (photon absorption cross sections), transition state entropy ($\Delta S^\ddagger$), and binding energy ($E_o$) on the measured dissociation kinetics. A master equation formalism, described elsewhere,[48] can be used for this purpose. Briefly, Einstein coefficients for radiative processes are calculated from theoretical vibrational frequencies and intensities. These are combined with a Planck distribution at the temperature of the copper jacket surrounding the ion cell to calculate photoactivation/deactivation rates. Dissociation is included in the simulation via sets of RRKM microcanonical dissociation rate constants calculated using a range of $E_o$ and $\Delta S^\ddagger$ values. If kinetic data is available at several temperatures, a master equation analysis may be used to determine dissociation energies.

For these experiments, a full analysis to determine dissociation energies was not done. The primary reason for this is uncertainty in the radiative energy density for experiments with a cooled ion cell. Although the radiation emitted from the copper jacket surrounding the ion cell can be described by a temperature, there are several holes in the jacket. These allow radiation from other sources that are not directly cooled to enter the ion cell and interact with the ions. An analysis of these effects is underway.[44] Qualitatively, the effective temperature experienced by the ions is higher than the temperature of the copper jacket. The lower the temperature of the copper jacket, the greater the discrepancy between measured and effective temperature. This results in measured activation energies that are artificially low. Here, we do a master equation analysis of a limited set of kinetic data measured at just a few temperatures. This analysis is intended to obtain a semiquantitative estimate of binding-energy differences of water to the different isomeric complexes of all three metal ions.

Results from the master equation analysis of the Val·M$^+$-(H$_2$O)$_2$ kinetics data are listed in Table 7. Again, we would like to stress the approximate nature of this analysis; these rough calculations were performed in order to assess the effects of dissociation parameters on the BIRD rate rather than to determine the exact range of dissociation energies for the loss of water. The dissociation energies calculated for the loss of the second water molecule is quite small, ranging from ~7 kcal/mol for the potassiated clusters to ~17 kcal/mol for the lithiated clusters. These dissociation energies are reasonable for the clusters studied based on the coordination state of Li$^+$, although the energies listed for the sodiated and potassiated clusters are almost certainly somewhat lower than the true dissociation energies for the reason discussed above. The dissociation energy for Val·Li$^+$(H$_2$O)$_{2\rightarrow1}$ is in good agreement with the dissociation energy for the reaction Li$^+$(H$_2$O)$_{4\rightarrow3}$, determined to be 17 kcal/mol by Armentrout and co-workers, assuming a loose transition state.[49] The dissociation energy for the potassiated clusters is somewhat higher than the ~5 kcal/mol binding of the water dimer. The modeled dissociation depends on the cluster's photon absorption/emission rates, $E_o$, and $\Delta S^\ddagger$. The effect of each of these parameters on the modeled dissociation rate is discussed below.

**Radiative Rates.** In our previous report, we used a master equation analysis to simulate the dissociation of all four AA's and found that the identity of the AA (and hence the calculated vibrational frequencies and radiative absorption intensities) had only a moderate effect on the dissociation rate constant. Given the same dissociation parameters ($E_o$ and $\Delta S^\ddagger$), the calculated dissociation rate for clusters containing the four isomers differed by 0−10%.[42] Similar calculations done for the larger clusters considered in this work also resulted in a variance of up to ~10%. This indicates that differences in experimentally measured rate constants greater than ~10% are not merely due to differential infrared absorption rates. Rather, large differences in kinetic rates result from differences in the dissociation parameters, $E_o$ and $\Delta S^\ddagger$. Modeled dissociation rates of different conformers of the same AA and of VN vs VZ are even more similar, generally within 5%. The similarity in absorption rates simplifies the modeling. In this report, we will focus on the modeling results from only one AA·M$^+$(H$_2$O)$_n$ conformer for each of the clusters. Although photoactivation rates do not change much between isomers (as was the intent in the choice of AlaOEt and Bet for models of valine), the dissociation rate measured depends strongly on the infrared absorption rates. Decreasing the modeled photon absorption rates by 10% decreases the modeled dissociation rate by ~9%.

**Transition State Entropy.** The effect of $\Delta S^\ddagger$ on dissociation rates is relatively small, and it depends on the metal ion size. The exact entropy of the transition state is not known for these reactions. For example, the entropy for loss of water from interconverting zwitterion and nonzwitterion forms of valine would be expected to differ somewhat from the entropy for loss of water from either Bet or AlaOEt. However, the loss of water should not be a geometrically constrained reaction for any of these isomers, and thus, the transition state is expected to be quite loose.

Table 7 lists dissociation rates of water from AA·M$^+$(H$_2$O)$_2$ calculated for $\Delta S^\ddagger$ corresponding to a "loose" (Arrhenius A factor of $10^{17}$ s$^{-1}$) and a "neutral" (Arrhenius A factor of $10^{13}$ s$^{-1}$) transition state. This wide range of transition state entropies is used to bracket the value that one would expect for these reactions. For M = Li, changing the modeled transition state from "loose" to "neutral" decreases the modeled dissociation rate constant by ~40%. For M = Na, the effect is much smaller (~15%). For M = K, the modeled dissociation rate is the same for the "neutral" and "loose" transition states. These results

indicate that the dissociation process for the potassiated cluster is in the so-called "truncated-Boltzmann" or "sudden death" limit in which the rate-limiting step for dissociation is the activation above the threshold energy. The sodiated clusters are close to this limit. Thus, for the clusters containing the larger metal ions, the results of the BIRD experiment are not expected to depend significantly on $\Delta S^{\ddagger}$.

For the AA·$Li^+(H_2O)_2$ clusters, the effect of transition state entropy is not inconsequential. However, it alone cannot account for the measured differences in the kinetics. The measured difference in rates between Val·$Li^+(H_2O)_{2\rightarrow1}$ and Bet·$Li^+(H_2O)_{2\rightarrow1}$ is 50% (Table 1) compared to the 40% maximum modeled difference due to wide difference in $\Delta S^{\ddagger}$ (Table 7). This 40% is a high estimate for the effect on rates because the transition state for dissociation should be looser than that modeled with an Arrhenius preexponential of $10^{13}$ $s^{-1}$. In addition, water bound in a fashion similar to different isomers ought to have similar $\Delta S^{\ddagger}$, although one may argue that the transition state of Bet and VN clusters may be slightly different because of their differing electronic configurations. Furthermore, although differences in $\Delta S^{\ddagger}$ could account for a portion of the difference in measured AA·$Li^+(H_2O)_2$ dissociation rates at a single temperature, it cannot account for the measured temperature dependence of the relative rates. This is discussed below.

**Dissociation Energy.** For all of the AA·$M^+(H_2O)_2$ clusters, kinetic data were measured at two or three different temperatures. By combining an Arrhenius analysis of the limited temperature-dependent data with the master equation analysis, approximate values of the dissociation energy were obtained using procedures described elsewhere.[48,50]

In addition to the kinetic data measured at 55 °C shown in Figure 1a, relative kinetics for AA·$Li^+(H_2O)_{2\rightarrow1}$ were also measured at room temperature. The activation energies determined from the Arrhenius analysis of these data are ~9 kcal/mol for AA = Val and AlaOEt and ~11 kcal/mol for AA = Bet. The similarity of the Val and AlaOEt activation energies indicates that these two isomers have similar dissociation energies, whereas the dissociation energy of the Bet cluster is somewhat higher. The range of dissociation energies determined by the master equation analysis of the Arrhenius data is 16−17 kcal/mol for AA = Val and AlaOEt and 17−18 kcal/mol for AA = Bet. This span of dissociation energies takes into account a wide range of transition state entropies, with Arrhenius A factors ranging from $10^{13}$ to $10^{17}$ $s^{-1}$. Although the range of dissociation energies determined for Val·$Li^+(H_2O)_2$ and Bet·$Li^+(H_2O)_2$ are very close, they do not overlap, even with the extremely large range of A factors modeled. Thus, the difference in measured kinetics reflects a difference in binding energy of water to the Val and Bet clusters.

For Val·$Na^+(H_2O)_2$, kinetic data was measured at three nominal temperatures, ranging from 0 to 55 °C. The span of dissociation energies determined from the master equation analysis of these data was ~11−13 kcal/mol. For Val·$K^+(H_2O)_2$, the dissociation energy determined from kinetic data at nominal temperatures of −50 and −100 °C is ~7−8 kcal/mol.

The dissociation rates are extremely sensitive to $E_o$, especially for the more weakly bound clusters. For M = Li, decreasing the modeled binding energy by 2.3 kcal/mol doubles the dissociation rate. For M = Na, a 1.4 kcal/mol decrease in binding energy doubles the dissociation rate. For M = K, a difference of just 0.8 kcal/mol doubles the rate. Thus, differences in the measured kinetics for extremely weakly bound clusters, such as those measured for AA·$K^+(H_2O)_2$, reflect extremely small differences in binding energy. Therefore, differences in relative kinetics measured for more strongly bound clusters have more structural significance than those measured for the more weakly bound clusters.

Taken together, the master equation analysis results indicate that dissociation kinetics are an extremely sensitive probe of binding energy for these clusters. For the more tightly bound lithiated clusters, differences in dissociation entropy have a moderate effect on kinetics, but it is not large enough alone to account for experimentally observed rated differences. For the less tightly bound sodiated and potassiated clusters, entropy effects are not significant. As the cluster size increases, the water binding energy decreases, whereas photon absorption rates increase slightly. Thus, for the clusters of higher hydration number, the dissociation rate should not depend significantly on the entropy of the transition state. For these clusters, the relative dissociation kinetics should be a more direct probe of binding energy. However, when binding is too weak, extremely small differences in binding energy result in large differences in kinetics. This complicates structural interpretation of the weakly bound clusters.

## Conclusions

The combined experimental and theoretical results indicate that only a few water molecules are necessary to transform Val·$M^+$ from its gas-phase to its solution-phase structure. For Val·$Li^+(H_2O)_2$, the metal ion is coordinated to both the nitrogen and carbonyl oxygen of the valine. The two water molecules interact solely with the metal ion. Upon the addition of a third water molecule, both experiment and theory indicate that the position of the metal ion changes. The most likely structure for Val·$Li^+(H_2O)_3$ is one in which valine adopts a zwitterionic form. Lithium binds to the C-terminal end of the valine, and again two water molecules interact with the lithium. The third water molecule interacts with the protonated N terminus of the valine. Thus, the first water molecule that interacts directly with the valine and not the metal can stabilize the zwitterionic form.

For M = Na, the change in the position of the metal ion from NO to OO coordination occurs at $n = 2$. Again, the theoretical results are consistent with experiment for this cluster. Theory predicts that the third water molecule interacts solely with the metal ion, leaving the structure of the cluster essentially unchanged from that for $n = 2$. However, this is inconsistent with experimental results which indicate that the mode of coordination of the third water molecule does not resemble the binding in any of the model clusters. Candidate conformations containing both nonzwitterionic and zwitterionic valine exist for this cluster. Thus, we are unable to determine the form of valine in Val·$Na^+(H_2O)_3$.

For M = K, dissociation kinetics indicate that the structure of Val·$K^+(H_2O)_2$ is not well mimicked by either of the model compounds. This suggests that the second water molecule does not interact with the metal ion but rather with the valine itself. All candidate structures for which this is true contain zwitterionic valine. Thus, the experimental results suggest that Val·$K^+(H_2O)_2$ contains the zwitterionic form of valine. However, the binding energy of the second water molecule to this cluster is extremely small, only slightly larger than a typical hydrogen bond. Thus, structural information inferred from kinetic experiments in such weakly bound clusters is only tentative.

It is difficult to draw structural conclusions for clusters with higher states of hydration. In part, this is because the models we have chosen no longer mimic all of the favorable Val−metal-ion−$H_2O$ interactions. A further complication is that the clusters have multiple weak water-binding sites, primarily sites

to which hydrogen bonds can form. Thus, similar kinetics in weakly bound clusters, though reflecting comparable binding energies, do not imply conformational resemblance. It is also likely that barriers to interconversion between structures are lower with increasing extents of hydration and that many conformers are populated under the conditions of the experiment.

An intriguing result from this series of experiments is that the sixth water molecule dissociates more slowly than the fifth water molecule in the Val·$M^+$ clusters for M = Li and Na. This indicates that the sixth water molecule is bound more strongly than the fifth in these clusters. It is possible that the binding of the fifth water introduces some strain in the backbone in order to maximize hydrogen-bonding interactions and that the addition of the sixth water molecule relieves this strain. This "magic number" provides further support for zwitterionic valine.

This study indicates that only a few water molecules are necessary to convert the most favorable gas-phase structure of an amino acid into the most stable form in bulk water. This result suggests that the gap in the understanding of the differences between gas-phase and solution-phase structure can be bridged by the study of hydrated gas-phase ions as a function of the number of water molecules attached. Studies such as these will help determine how water effects biomolecule structure.

**Acknowledgment.** Financial support was provided by the National Science Foundation (Grant CHE-0098109). This work was partially supported by the National Computational Science Alliance under CHE010013N and utilized the NCSA SGI/CRAY Orgin2000.

**Supporting Information Available:** Nuclear coordinates (Table S1). This material is available free of charge via the Internet at http://pubs.acs.org.

## References and Notes

(1) Creighton, T. E. *Proteins: Structures and Molecular Properties*, 2nd ed.; W. H. Freeman & Co.: New York, 1993.
(2) Klibanov, A. M. *Nature* **2001**, *409*, 241−246.
(3) Covey, T.; Douglas, D. J. *J. Am. Soc. Mass Spectrom.* **1993**, *4*, 616−623.
(4) Gross, D. S.; Schnier, P. D.; Rodriguez-Cruz, S. E.; Fagerquist, C. K.; Williams, E. R. *Proc. Natl. Acad. Sci. U.S.A.* **1996**, *93*, 3143−3148.
(5) Shelimov, K. B.; Clemmer, D. E.; Hudgins, R. R.; Jarrold, M. F. *J. Am. Chem. Soc.* **1997**, *119*, 2240−2248.
(6) McLafferty, F. W.; Guan, Z. Q.; Haupts, U.; Wood, T. D.; Kelleher, N. L. *J. Am. Chem. Soc.* **1998**, *120*, 4732−4740.
(7) Matthews, B. W. *Acc. Chem. Res.* **1988**, *21*, 333−340.
(8) Chakrabartty, A.; Baldwin, R. L. *Adv. Protein Chem.* **1995**, *46*, 141−176.
(9) Hudgins, R. R.; Mao, Y.; Ratner, M. A.; Jarrold, M. F. *Biophys. J.* **1999**, *76*, 1591−1597.
(10) Kohtani, M.; Kinnear, B. S.; Jarrold, M. F. *J. Am. Chem. Soc.* **2000**, *122*, 12377−12378.
(11) Schnier, P. D.; Klassen, J. S.; Strittmatter, E. E.; Williams, E. R. *J. Am. Chem. Soc.* **1998**, *120*, 9605−9613.
(12) Loo, J. A.; He, J. X.; Cody, W. L. *J. Am. Chem. Soc.* **1998**, *120*, 4542−4543.
(13) Rostom, A. A.; Fucini, P.; Benjamin, D. R.; Juenemann, R.; Nierhaus, K. H.; Hartl, F. U.; Dobson, C. M.; Robinson, C. V. *Proc. Natl. Acad. Sci. U.S.A.* **2000**, *97*, 5185−5190.
(14) Chowdhury, S. K.; Katta, V.; Chait, B. T. *Rapid Commun. Mass Spectrom.* **1990**, *4*, 81−87.
(15) Rodriguez-Cruz, S. E.; Klassen, J. S.; Williams, E. R. *J. Am. Soc. Mass Spectrom.* **1997**, *8*, 565−568.
(16) Lee, S. W.; Freivogel, P.; Schindler, T.; Beauchamp, J. L. *J. Am. Chem. Soc.* **1998**, *120*, 11758−11765.
(17) Yu, D.; Armstrong, D. A.; Rauk, A. *Can. J. Chem.* **1992**, *70*, 1762−1772.
(18) Jensen, J. H.; Gordon, M. S. *J. Am. Chem. Soc.* **1991**, *113*, 7917−7924.
(19) Ding, Y. B.; Krogh-Jespersen, K. *Chem. Phys. Lett.* **1992**, *199*, 261−266.
(20) Jensen, J. H.; Gordon, M. S. *J. Am. Chem. Soc.* **1995**, *117*, 8159−8170.
(21) Suenram, R. D.; Lovas, F. J. *J. Mol. Spectrosc.* **1978**, *72*, 372−382.
(22) Locke, M. J.; McIver, R. T., Jr. *J. Am. Chem. Soc.* **1983**, *105*, 4226−4232.
(23) Iijima, K.; Tanaka, K.; Onuma, S. *J. Mol. Struct.* **1991**, *246*, 257−266.
(24) Price, W. D.; Jockusch, R. A.; Williams, E. R. *J. Am. Chem. Soc.* **1997**, *119*, 11988−11989.
(25) Maksic, Z. B.; Kovacevic, B. *J. Chem. Soc., Perkin Trans. 2* **1999**, 2623−2629.
(26) Chapo, C. J.; Paul, J. B.; Provencal, R. A.; Roth, K.; Saykally, R. J. *J. Am. Chem. Soc.* **1998**, *120*, 12956−12957.
(27) Jensen, F. *J. Am. Chem. Soc.* **1992**, *114*, 9533−9537.
(28) Hoyau, S.; Ohanessian, G. *Chem. Eur. J.* **1998**, *4*, 1561−1569.
(29) Wyttenbach, T.; Bushnell, J. E.; Bowers, M. T. *J. Am. Chem. Soc.* **1998**, *120*, 5098−5103.
(30) Wyttenbach, T.; Witt, M.; Bowers, M. T. *J. Am. Chem. Soc.* **2000**, *122*, 3458−3464.
(31) Jockusch, R. A.; Price, W. D.; Williams, E. R. *J. Phys. Chem. A* **1999**, *103*, 9266−9274.
(32) Kassab, E.; Langlet, J.; Evleth, E.; Akacem, Y. *J. Mol. Struct. (THEOCHEM)* **2000**, *531*, 267−282.
(33) Tajkhorshid, E.; Jalkanen, K. J.; Suhai, S. *J. Phys. Chem. B* **1998**, *102*, 5899−5913.
(34) Klassen, J. S.; Blades, A. T.; Kebarle, P. *J. Phys. Chem.* **1995**, *99*, 15509−15517.
(35) Mautner, M. M. N.; Elmore, D. E.; Scheiner, S. *J. Am. Chem. Soc.* **1999**, *121*, 7625−7635.
(36) Robertson, E. G.; Hockridge, M. R.; Jelfs, P. D.; Simons, J. P. *J. Phys. Chem. A* **2000**, *104*, 11714−11724.
(37) Mons, M.; Dimicoli, I.; Tardivel, B.; Piuzzi, F.; Robertson, E. G.; Simons, J. P. *J. Phys. Chem. A* **2001**, *105*, 969−973.
(38) Robertson, E. G.; Hockridge, M. R.; Jelfs, P. D.; Simons, J. P. *Phys. Chem. Chem. Phys.* **2001**, *3*, 786−795.
(39) Robertson, E. G.; Simons, J. P. *Phys. Chem. Chem. Phys.* **2001**, *3*, 1−18.
(40) Carney, J. R.; Fedorov, A. V.; Cable, J. R.; Zwier, T. S. *J. Phys. Chem. A* **2001**, *105*, 3487−3497.
(41) Mao, Y.; Ratner, M. A.; Jarrold, M. F. *J. Am. Chem. Soc.* **2000**, *122*, 2950−2951.
(42) Jockusch, R. A.; Lemoff, A. S.; Williams, E. R. *J. Am. Chem. Soc.* In press.
(43) Price, W. D.; Schnier, P. D.; Williams, E. R. *Anal. Chem.* **1996**, *68*, 859−866.
(44) Wong, R. L.; Williams, E. R. Manuscript in preparation.
(45) Hay, P. J.; Wadt, W. R. *J. Phys. Chem.* **1985**, *82*, 299−310.
(46) Feller, D.; Glendening, E. D.; Kendall, R. A.; Peterson, K. A. *J. Chem. Phys.* **1994**, *100*, 4981−4997.
(47) Feller, D.; Glendening, E. D.; Woon, D. E.; Feyereisen, M. W. *J. Chem. Phys.* **1995**, *103*, 3526−3542.
(48) Price, W. D.; Schnier, P. D.; Williams, E. R. *J. Phys. Chem. B* **1997**, *101*, 664−673.
(49) Rodgers, M. T.; Armentrout, P. B. *J. Phys. Chem. A* **1997**, *101*, 1238−1249.
(50) Jockusch, R. A.; Williams, E. R. *J. Phys. Chem. A* **1998**, *102*, 4543−4550.